ELSEVIER

Available online at www.sciencedirect.com
SCIENCE DIRECT®

Theoretical and Applied Fracture Mechanics 42 (2004) 295–301

theoretical and applied fracture mechanics

www.elsevier.com/locate/tafmec

Defect nucleation in SOI wafers due to hydrogen ion implantation

M. Xu, X.Q. Feng *

Key Lab of Failure Mechanics of Education Ministry, Department of Engineering Mechanics, Tsinghua University, Beijing 100084, China

Available online 5 November 2004

Abstract

Hydrogen ion implantation in the Smart-Cut production process leads to fracture of Si–Si bonds, formation of microcavities and splitting of a single-crystal silicon wafer. In the present paper, an analysis model for defect nucleation induced by hydrogen ion implantation is established based on the continuum mechanics theory accounting for the crystal structure of silicon. Using this model and probability theory, an analytical expression is derived to calculate the defect density as a function of the hydrogen ion implantation dose and the temperature.
© 2004 Elsevier Ltd. All rights reserved.

Keywords: Hydrogen ion implantation; Silicon-on-insulator; Smart-Cut technology; Defect nucleation; Nanomechanics; Fracture

1. Introduction

Processing and manufacturing requirements for ultra-large-scale integration (ULSI) device structures have enabled rapid development of the silicon-on-insulator (SOI) semiconductor industry. A typical SOI system consists of a thin layer of single-crystal silicon supported by an underlying insulator (e.g., SiO_2 and sapphire). SOI technology has substantial advantages over traditional bulk Si processing for a wide range of ULSI applications [1–4]. SOI-based integrated circuits possess such advantages as high speeds, high packing density, immunity from latch-up, low power dissipation and high resistance to ionizing radiation. Smart-Cut® technology is a promising technology recently developed by Bruel and his co-workers to fabricate high quality SOI structures [5–7]. This technology combines skillfully hydrogen ion implantation and wafer bonding, and it seems to meet all the requirements for ULSI applications.

Since the first publication [5,6], the Smart-Cut technique has attracted increasingly extensive attentions and has found practical applications in

* Corresponding author. Tel.: +86 10 6277 2934; fax: +86 10 6278 1824.
E-mail address: fengxq@tsinghua.edu.cn (X.Q. Feng).

0167-8442/$ - see front matter © 2004 Elsevier Ltd. All rights reserved.
doi:10.1016/j.tafmec.2004.09.004

the field of SOI. This technique has already in 1997 been used in the industrial production of SOI structures [7,8]. Successful applications of the Smart-Cut technique for production of SOI structures have stimulated a great interest to develop this method for synthesizing other layered and even three-dimensional structures of semiconductors. It was demonstrated in [9] that the Smart-Cut technology could be used for the production of "SiC-on-insulator" structures. In [10], Si, Ge, and GaAs films were transformed on substrates of a high-melting glass. The feasibility of applying the Smart-Cut technology to structured and patterned thin silicon films has also been demonstrated. Some new structures with thin films of Si, GaAs or InP on silicon substrates have been obtained by using the Smart-Cut technique combined with metal bonding [7,11,12]. GaSb-on-insulator structures formed on GaAs substrates and the novel silicon-on-aluminum-nitride (SOAN) structure were realized recently by the ion-cut process using hydrogen ion implantation [13].

Though the Smart-Cut technology has had some successful applications, its underlying physical mechanisms have not been well understood. The fundamental understanding of the basic mechanisms of the Smart-Cut production process will benefit the further process development and large-scale implementation of the technique. In the present paper, attention will be focused on the physical mechanisms of defect nucleation and evolution in silicon wafers due to hydrogen ion implantation, which is the most significant process step of the Smart-Cut technology. A model for defect nucleation due to hydrogen implantation will be presented based on the elasticity theory with the crystalline structure of silicon being taken into account. Then based on a statistical analysis of probability theory, the defect density is estimated as a function of implantation dose and annealing temperature.

2. Nucleation of a porous layer in a silicon wafer

2.1. *Effects of hydrogen on defect nucleation*

Two significant ideas of the Smart-Cut technology are to acquire a large number of microdefects (microcracks and microvoids) concentrated in a very thin layer in the silicon wafer by hydrogen ion implantation and to split the wafer system later by thermal annealing. Therefore, an insight into the nucleation of microcavities associated with hydrogen implantation is of interest. Chemical, physical and mechanical considerations are all necessary in order to gain a fundamental understanding of this complicated process occurred at the nanometer scale involving chemical reaction, bond decohesion, and mechanical deformation and fracture. After the hydrogen implantation, the trapped hydrogen atoms or protons combine with silicon atoms to form Si–H bonds. The energy needed is supplied either by thermal energy at a high temperature during annealing or by mechanical energy (elastic strain energy) stored in the compound system due to high residual stress (or internal pressure) caused by hydrogen implantation. Microcavity nucleation starts mainly at the late stage of hydrogen implantation and is accelerated by the subsequent thermal treatment. During hydrogen ion implantation at room temperature, the elastic strain energy induced by residual stress plays a predominant role in fracture of Si–Si bonds. On the other hand, during high temperature annealing, both thermal and mechanical energy make significant contributions to the fracture process.

A knowledge of the silicon's crystalline structure is useful to the understanding of the defect nucleation process. Silicon possesses a cubic crys-

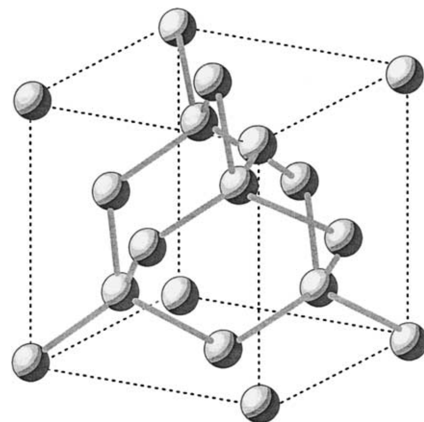

Fig. 1. A cubic unit cell of crystalline structure of Si.

tal structure of diamond, as shown in Fig. 1. The parameters of the unit cell include the lengths $a = b = c = 0.54309$ nm and the angles $\alpha = \beta = \gamma = 90°$. The Si–Si bond length is 0.2352 nm. The unit cell can be divided into eight cube-shaped sub-cells of same size, with the edge length being $a/2$. Each of the four sub-cells with centers located at $(\frac{3}{4}a, \frac{1}{4}b, \frac{1}{4}c)$, $(\frac{1}{4}a, \frac{3}{4}b, \frac{1}{4}c)$, $(\frac{1}{4}a, \frac{1}{4}b, \frac{3}{4}c)$ and $(\frac{3}{4}a, \frac{3}{4}b, \frac{3}{4}c)$ has a body-centered Si atom whereas the other four sub-cells have not. This means that in each unit cell of silicon crystal there are four intrinsic voids (interstitial spacing vacancies) with centers at $(\frac{1}{4}a, \frac{3}{4}b, \frac{3}{4}c)$, $(\frac{3}{4}a, \frac{1}{4}b, \frac{3}{4}c)$, $(\frac{3}{4}a, \frac{3}{4}b, \frac{1}{4}c)$ and $(\frac{1}{4}a, \frac{1}{4}b, \frac{1}{4}c)$, respectively. The void size, to be given below, is comparable to a Si atom but is much larger than a hydrogen ion. Therefore, most hydrogen ions implanted are trapped in these inherent voids, which serve as sources of larger defects. Hydrogen within such an intrinsic vacancy may form hydrogen molecules [14].

Though the overall implanted system is traction free, the internal pressure of hydrogen gas induces residual stress at the nanometer scale, and therefore provides elastic strain energy for fracture of Si–Si bonds, as discussed earlier. The implantation process pushes more and more hydrogen ions into the voids, causing the increase of internal pressure in the voids. The trapped hydrogen atoms diffuse and segregate near the peak implantation region during thermal annealing, forming microvoids filled with H_2 molecules, the high pressure inside the microcavities, which is magnified significantly due to the high temperature in thermal annealing, is the driving force for nucleation and expansion of defects.

It is well known that single-crystal silicon has a relatively high strength, with a theoretical strength about 7 GPa. However, the implanted hydrogen has an embrittlement effect, which significantly lowers the fracture stress of silicon. The hydrogen ions or molecules may react with silicon to form Si–H bonds following fracture of Si–Si bonds. The embrittlement effect of hydrogen also depends strongly on temperature. Therefore, there exist two synergistic physical mechanisms by which the implantation of hydrogen may induce nucleation and growth of nano-sized defects in a silicon wafer, namely, the internal pressure of molecule hydrogen in microvoids to provide the driving force for fracture of Si–Si bonds and the hydrogen embrittlement effect to significantly reduce the fracture resistance.

Such a nucleation process occurs at the nanometer scale and involves complex physical and chemical mechanisms, atomistic studies such as molecular dynamic simulation seem appropriate to investigate the microstructure evolution of a silicon wafer during hydrogen implantation and the subsequent thermal annealing. However, atomistic studies are generally very time-consuming due to the relatively large size and relatively long time involved in the Smart-Cut process. To gain a fundamental and quantitative understanding of defect nucleation and evolution, therefore, we present in the following subsection a model based on continuum mechanics theory with atomistic structure of single-crystal silicon being considered. Similar hybrid atomistic/continuum models have been investigated and used recently in [15–17].

2.2. Model for defect nucleation

Single-crystal silicon wafers currently adopted for SOI devices are generally of high quality and have few defects. Therefore, it is reasonable to assume that all the defects are induced merely by hydrogen implantation. Consider an intrinsic void in the silicon crystal filled by hydrogen ions and/or molecules. According to crystalline structure in Fig. 1, the void radius R_0 can be estimated from the crystal lattice parameter a as:

$$R_0 = \sqrt{3}a/8 = 0.1176 \text{ nm}, \tag{1}$$

which is comparable to the silicon atom radius (0.110 nm) but much larger (140 times in volume) than the hydrogen atom radius (0.025 nm). The hydrogen molecules contained in these intrinsic vacancies have been modeled as gas by Freund [18], Varma [19] and some others. The hydrogen-induced internal pressure p in the void is governed approximately by the following equation for a perfect gas:

$$pV = n_{H_2}\kappa T, \tag{2}$$

where V is the void volume, n_{H_2} is the number of hydrogen molecules, T is the absolute temperature,

and $\kappa = 1.38065 \times 10^{-23}$ J K^{-1} is the Boltzmann's constant.

Because of its cubic crystal structure, the single-crystal silicon is treated as a linearly elastic and isotropic material with Young's modulus E and Poisson's ratio v. At the early stage of defect nucleation, the volume fraction of defects is very small such that the effect of defect interaction is negligible and we may consider a spherical void subjected to an internal pressure p in an infinite elastic matrix. The linear elasticity solution gives the nonzero stress and displacement components in a spherical coordinate system (r, θ, φ) as

$$\sigma_r = -\frac{pR^3}{r^3}, \quad \sigma_\theta = \sigma_\varphi = \frac{pR^3}{2r^3}, \tag{3}$$

$$u_r = \frac{(1+v)pR^3}{2Er^2}, \tag{4}$$

respectively, where R is the void radius after deformation due to the internal pressure, and r the distance from the void center. Note that the void radius R may be significantly different from its initial radius R_0 (prior to deformation) due to the high pressure p responsible for fracture of Si–Si bonds. Therefore, we use the radius R after deformation in Eqs. (3) and (4) to account for this effect of void radius.

Then the void radius R is obtained from Eq. (4) as

$$R = R_0 + u_r|_{r=R} = R_0\left[1 - \frac{(1+v)p}{2E}\right]^{-1}. \tag{5}$$

Then the void volume after deformation is written as

$$V = \frac{4\pi}{3}R^3 = \frac{4\pi R_0^3}{3}\left[1 - \frac{(1+v)p}{2E}\right]^{-3}. \tag{6}$$

Its substitution into (2) gives the governing equation for the internal pressure p,

$$\frac{4\pi R_0^3 p}{3}\left[1 - \frac{(1+v)p}{2E}\right]^{-3} = n_{H_2}\kappa T, \tag{7}$$

which has the following solution for p in term of the number of hydrogen molecules n_{H_2} and temperature T:

$$p = \left[\frac{4\pi R_0^3}{3} + \frac{3n_{H_2}\kappa T(1+v)}{2E}\right]^{-1} n_{H_2}\kappa T, \tag{8}$$

under the assumption that the internal pressure p is much less than the Young's modulus E. Thus, the maximum circumferential tensile stress at the boundary of the void is given by [15]

$$\sigma_{\max} = \sigma_\theta|_{r=R} = n_{H_2}\kappa T\left[\frac{8\pi R_0^3}{3} + \frac{3n_{H_2}\kappa T(1+v)}{E}\right]^{-1}. \tag{9}$$

Owing to the brittleness of silicon, we take a maximum tensile stress criterion of defect nucleation:

$$\sigma_{\max} = \sigma_c, \tag{10}$$

where σ_c is the fracture stress of silicon, and is significantly lower than the theoretical fracture stress due to the hydrogen embrittlement effect. The dependence of σ_c upon the hydrogen ion density and temperature is still an open problem and is beyond the scope of this paper.

Eqs. (9) and (10) give the critical number of hydrogen molecules for defect nucleation (fracture of Si–Si bonds):

$$n_{H_2}^c = \frac{8\pi R_0^3\sigma_c}{3\kappa T}\left[1 - \frac{3(1+v)\sigma_c}{E}\right]^{-1}. \tag{11}$$

Examine the critical number $n_{H_2}^c$ of hydrogen molecules for the following representative parameters: Boltzmann's constant $\kappa = 1.38065 \times 10^{-23}$ J K^{-1}, radius $R_0 = 0.1176$nm, Young's modulus $E = 166$GPa, Poisson's ratio $v = 0.17$, fracture stress $\sigma_c = 1.0$GPa. Consider temperatures $T =$ 298 and 773 K, corresponding respectively to the room-temperature (25 °C) and thermal annealing (500 °C). These give $n_{H_2}^c$ as 3.2 at room temperature and 1.2 at thermal annealing. This suggests that at room temperature (25 °C), a defect will form at the position of an intrinsic vacancy if four or more hydrogen molecules are located in it. According to the theory of statistics and probability, the density of vacancies having two or more hydrogen molecules is much bigger than that of vacancies having four or more hydrogen mole-

cules. Therefore, thermal treatment will accelerate the defect nucleation process by many times, as will be shown later.

3. Defect density

3.1. Calculation model of defect density

The implantation dose D_H of hydrogen ions in industrial production is generally in the range between 3.5×10^{16} and 1.0×10^{17} cm^{-2}. Experimental observations [7] shown that most hydrogen ions are concentrated in a thin layer with thickness t_H in the range of 100–200 nm. The average number of hydrogen ions implanted in each void is

$$n_H = \frac{D_H}{t_H n_{void}}. \quad (12)$$

If we take the representative values $D_H = 1.0\times10^{17}$ cm^{-2}, $t_H = 100$ nm and $n_{void} = 2.498\times10^{22}$cm^{-3} calculated from the crystalline parameters of Si, we find that $n_H = 0.4$, which, as expected, is lower than the upper bound $2n^c_{H_2}$.

Based on the above analysis, estimate is made for the density of defects induced by implanted hydrogen ions, d_{defect}, which is defined as the number of intrinsic vacancies per unit area, resulting from fracture of Si–Si bonds [7]. Assume that all implanted hydrogen ions are randomly located in all the intrinsic voids of the peak-concentration layer. A defect forms at the site of a vacancy once the number of hydrogen ions in it reaches the critical value $2n^c_{H_2}$. Thus, the expected value of the defect density can be obtained either by a statistical analysis or Monte-Carlo simulation. Both the methods have been adopted in our study, and their results agree well. However, only the former is presented here because it may lead to a simple analytical solution.

For the problem that hydrogen ions of number $m_{ion} = D_H/t_H$ are completely randomly located in voids of number n_{void}, mathematically, the numbers of hydrogen ions (or "small balls") in each of the intrinsic vacancies (or "boxes") can be described by a multinomial distribution. Denote X_i as the number of hydrogen ions in the ith vacancy. The probability for $X_i = k_i$ is given by [20]

$$P(X_1 = k_1, \ldots, X_{n_{void}} = k_{n_{void}}) = \frac{m_{ion}!}{k_1!\cdots k_{n_{void}}!}\left(\frac{1}{n_{void}}\right)^{k_1}\left(\frac{1}{n_{void}}\right)^{k_2}\cdots\left(\frac{1}{n_{void}}\right)^{k_{n_{void}}}, \quad (13)$$

where

$$k_i \geqslant 0, \quad k_1 + k_2 + \cdots + k_{n_{void}} = m_{ion}. \quad (14)$$

Substitution of Eq. (14) into (13) leads to

$$P(X_1 = k_1, \ldots, X_{n_{void}} = k_{n_{void}}) = \frac{m_{ion}!}{k_1!\cdots k_{n_{void}}!}\left(\frac{1}{n_{void}}\right)^{m_{ion}}. \quad (15)$$

The number of the "boxes", each of which contains more than x balls, is designated as a function $S(m_{ion}, n_{void}, x) = \sum_{\alpha=1}^{n_{void}} I_{(X_\alpha > x)}$, where $I_{(X_\alpha > x)}$ is the characteristic function of X_α and defined as $I_{(X_\alpha > x)} = 1$ and 0 for $X_\alpha > x$ and $X_\alpha \leqslant x$, respectively. The mathematical expectation of $S(m_{ion}, n_{void}, x)$ is given by

$$E[S(m_{ion}, n_{void}, x)] = E\left(\sum_{\alpha=1}^{n_{void}} I_{(X_\alpha > x)}\right) = \sum_{\alpha=1}^{n_{void}} P(X_\alpha > x) = n_{void} P(X_1 > x). \quad (16)$$

Then taking $x = 2n^c_{H_2} - 1$ in Eq. (16), the mathematical expectation value of the number density of voids that contains hydrogen ions more than $2n^c_{H_2}$ is derived as

$$d_{defect} = n_{void} t_H \left[1 - \sum_{\alpha=0}^{2n^c_{H_2}-1} C^\alpha_{m_{ion}} \left(\frac{1}{n_{void}}\right)^\alpha \times \left(\frac{n_{void}-1}{n_{void}}\right)^{m_{ion}-\alpha}\right]. \quad (17)$$

Since both n_{void} and m_{ion} are very large number and $m_{ion}/n_{void} < 1$, the number density of defects in Eq. (17) can be calculated more easily by

$$d_{defect} = n_{void} t_H \left[1 - \sum_{\alpha=0}^{2n^c_{H_2}-1} \frac{1}{\alpha!}\left(\frac{m_{ion}}{n_{void}}\right)^\alpha \exp\left(-\frac{m_{ion}}{n_{void}}\right)\right]. \quad (18)$$

3.2. Examples and discussions

Eq. (18) gives an analytical expression of the density function d_{defect} in a silicon wafer due to hydrogen implantation as a function of the implantation dose and the critical hydrogen molecule numbers, $n^{c}_{H_2}$, which depends mainly on temperature. Under various implantation doses, the defect densities are plotted in Fig. 2 with respect to $n^{c}_{H_2}$, where we take $t_H = 100$ nm. For easier estimation of defect density in SOI production, the dependence relation of the defect density $n^{c}_{H_2}$ can be approximated by a linear or polynomial empirical formula. By fitting the five curves in Fig. 2, the following formula is obtained:

$$\lg d_{\text{defect}} = 19.40 + 2n^{c}_{H_2}(6D_H \times 10^{-18} - 1.86), \tag{19}$$

which agrees reasonably with Eq. (18) in the range of implantation dose $3.5\text{–}10 \times 10^{16}\text{cm}^{-2}$. Eqs. (18) and (19) are compared in Fig. 3 for $D_H = 1.0 \times 10^{17}\text{cm}^{-2}$.

Thus, once the temperature (or the corresponding $n^{c}_{H_2}$) and the implantation dose D_H are given, the approximate defect density can be easily estimated from Eq. (19). In addition, Figs. 2 and 3 indicate a strong dependence of defect nucleation and evolution on temperature. For instance, it is estimated from Eq. (18) that the defect density at room temperature after implantation is only $2.88 \times 10^{9}\text{cm}^{-2}$ but reaches 1.95×10^{14} cm^{-2} at 500 °C during thermal annealing, that is, the defect nucleation is accelerated by about five orders by heating. The latter number of defect number density indicates that as a direct result of hydrogen ion implantation and thermal annealing, only a very small fraction of intrinsic vacancies (less than one percent) will undergo fracture of Si–Si bonds and become defects. In other words, the splitting of the SOI wafer is dominated by the subsequent growth and coalescence of these microdefects, which form microcracks. These two numbers agree reasonably well with the transmission scanning microscopy experimental observations [7], though they are slightly larger than the experimental data for several reasons discussed in the following. First, certain fractions of implanted hydrogen ions are located out of this thin layer, and do not cause defects. Second, if two or more neighboring vacancies form defects, they will coalesce to form a larger defect. Third, it is possible for hydrogen ions diffuse into a defect in its neighboring vacancies, and therefore the nucleation of a defect may impede nucleation of new defects in a small neighboring region. In addition, if two defects are very near in spacing, hydrogen ions or molecules may diffuse from one defect into another due to their possible difference in internal pressure. Thus one defect will expand while the other will shrink or even disappear. This is referred to as the Ostwald ripening

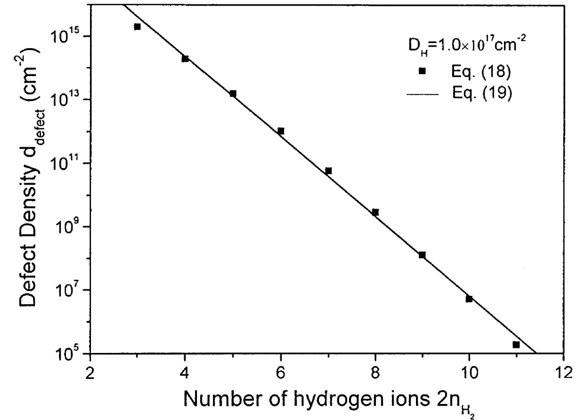

Fig. 3. Comparison of the defect density estimated from Eqs. (18) and (19) under $D_H = 1.0 \times 10^{17}$ cm^{-2}.

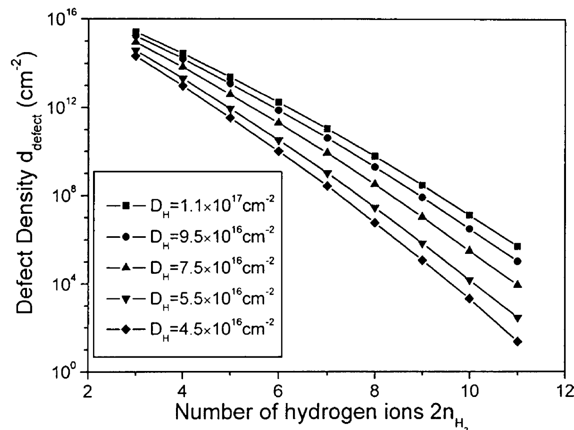

Fig. 2. Defect density with respect to the critical hydrogen ion number under different implantation doses of hydrogen ions.

mechanism [3], which also results in a decrease in the defect number that can be observed.

4. Conclusions

Hydrogen ion implantation has been applied in various microelectronics manufacturing processes such as Smart-Cut technology. This paper presents a fundamental study on some basic mechanisms associated with hydrogen ion implantation in SOI wafers from the mechanical and physical viewpoints. A model for defect nucleation induced by hydrogen ion implantation is established based on the continuum mechanics theory accounting for the effect of crystal structure of Si. An analytical expression is given for estimating the number density of defects. It is found that most defects nucleate in the stage of thermal annealing, which may accelerates the rate of defect nucleation by four or five orders of magnitude. Considered here is only the hydrogen ion implantation in SOI wafers. However, the present method seems of interest for analyzing other ion implantation processes.

Acknowledgments

The authors acknowledge the support from the National Natural Science Foundation of China (Grant Nr. 10028204 and 10102008) and the Education Ministry of China (National Excellent Doctoral Dissertation Funding Grant Nr. 199926; Key Grant Project Nr. 0306; and SRFDP Nr. 20030003067). XQF also thanks the support from the National 973 Project (2004CB619303).

References

[1] J.P. Colinge, Silicon-on-Insulator Technology: Materials to VLSI, Kluwer Academic, Boston, 1991.

[2] R.A. Yankov, S. Mändl, Plasma immersion ion implantation for silicon processing, Ann. Phys. Berlin 10 (2001) 279–298.

[3] J. Haisma, G.A.C.M. Spierings, Contact bonding, including direct-bonding in a historical and recent context of materials science and technology, physics and chemistry—Historical review in a broader scope and comparative outlook, Mater. Sci. Eng. R 37 (2002) 1–60.

[4] G.K. Celler, S. Cristoloveanu, Frontiers of silicon-on-insulator, J. Appl. Phys. 93 (2003) 4955–4978.

[5] M. Bruel, Silicon-on-insulator material technology, Electron. Lett. 31 (1995) 1201–1202.

[6] M. Bruel, Application of hydrogen ion beams to Silicon on Insulator material technology, Nucl. Instrum. Methods Phys. Res. B 108 (1996) 313–319.

[7] B. Aspar, M. Bruel, H. Moriceau et al., Basic mechanisms involved in the Smart-Cut(R) process, Microelectron. Engng. 36 (1997) 233–240.

[8] V.V. Kozlovskii, V.A. Kozlov, V.N. Lomasov, Modification of semiconductors with proton beams, Semiconductors 34 (2000) 129–147.

[9] L. Di Cioccio, F. Letertre et al., Silicon carbide on insulator formation by the Smart-Cut(R) process, Mater. Sci. Engng. B 46 (1997) 349–356.

[10] Q.Y. Tong, L.J. Huang, U.M. Gosele, Transfer of semiconductor and oxide films by wafer bonding and layer cutting, J. Electron. Mater. 29 (2000) 928–932.

[11] E. Jalaguier, B. Aspar, M. Bruel et al., Electron. Lett. 34 (1998) 408–409.

[12] Y. Zheng, P.D. Moran, Z.F. Guan et al., Transfer of 3 in GaAs film on silicon substrate by proton implantation process, J. Electron. Mater. 29 (2000) 916–920.

[13] Z.H. An, C.L. Men, X.Y. Xie et al., Fabrication of silicon-on-AlN novel structure and its residual strain characterization, J. Cryst. Growth 244 (2002) 27–32.

[14] M.K. Weldon, M. Collot, Y.J. Chabal et al., Mechanism of silicon exfoliation induced by hydrogen/helium co-implantation, Appl. Phys. Lett. 73 (1998) 3721–3723.

[15] X.Q. Feng, Y. Huang, Mechanics of Smart-Cut technology, Int. J. Solids Struct. 41 (2004) 4299–4320.

[16] H. Jiang, X.Q. Feng, Y. Huang et al., Defect nucleation in carbon nanotubes under tension and torsion: Stone–Wales transformation, Comput. Methods Appl. Mech. Engng. 193 (2004) 3419–3429.

[17] G.C. Sih, Implication of scaling hierarchy associated with nonequilibrium: field and particulate, Theoret. Appl. Fract. Mech. 37 (2001) 335–369.

[18] L.B. Freund, A lower bound on implant density to induce wafer splitting in forming compliant substrate structures, Appl. Phys. Lett. 70 (1997) 3519–3521.

[19] C.M. Varma, Hydrogen-implant induced exfoliation of silicon and other crystals, Appl. Phys. Lett. 71 (1997) 3519–3521.

[20] Y. Lin, Probability Mathematics, Tsinghua University Press, Beijing, 1999.